

---

# CIPER: COMBINING INVARIANT AND EQUIVARIANT REPRESENTATIONS USING CONTRASTIVE AND PREDICTIVE LEARNING

---

**Xia Xu\*, Jochen Triesch<sup>✉</sup>**  
 Frankfurt Institute for Advanced Studies  
 Frankfurt am Main, Germany  
 {xiaxu, triesch}@fias.uni-frankfurt.de

## ABSTRACT

Self-supervised representation learning (SSRL) methods have shown great success in computer vision. In recent studies, augmentation-based contrastive learning methods have been proposed for learning representations that are invariant or equivariant to pre-defined data augmentation operations. However, invariant or equivariant features favor only specific downstream tasks depending on the augmentations chosen. They may result in poor performance when a downstream task requires the counterpart of those features (e.g., when the task is to recognize hand-written digits while the model learns to be invariant to in-plane image rotations rendering it incapable of distinguishing “9” from “6”). This work introduces Contrastive Invariant and Predictive Equivariant Representation learning (CIPER). CIPER comprises both invariant and equivariant learning objectives using one shared encoder and two different output heads on top of the encoder. One output head is a projection head with a state-of-the-art contrastive objective to encourage invariance to augmentations. The other is a prediction head estimating the augmentation parameters, capturing equivariant features. Both heads are discarded after training and only the encoder is used for downstream tasks. We evaluate our method on static image tasks and time-augmented image datasets. Our results show that CIPER outperforms a baseline contrastive method on various tasks, especially when the downstream task requires the encoding of augmentation-related information.

**Keywords** self-supervised representation learning · contrastive learning · invariance learning · equivariance learning

## 1 Introduction

Recent advances in self-supervised representation learning (SSRL) have drawn much attention [1, 2, 3, 4] due to the performance comparable to supervised methods without the need for supervision. Essentially, without access to extra supervisory signals, SSRL utilizes internal structures of the data as supervisory information that is supposed to be well-encoded in the latent space. Among state-of-the-art SSRL methods, contrastive learning with deep neural network-based backbones can learn representations that perform well in various tasks [5, 6, 7, 8]. Much recent progress in contrastive learning has been made by introducing strong data augmentations which serve as an inductive bias to learn certain features. For example, a state-of-the-art contrastive learning framework, SimCLR [5], uses image data augmentations like random cropping, color jittering, and random horizontal flipping, assuming that these operations do not change the semantic meaning of an image with respect to, e.g., a downstream classification task. In contrastive learning, representations of the differently augmented versions of the same image are made similar. Hence the learned features would be encouraged to be invariant to the augmentations applied. Representations of different images (and their augmented versions) are made dissimilar to avoid representation collapse, preserving as much discriminative information as possible. The gist of modern contrastive learning can be interpreted as distinguishing images from each other while discarding augmentation-related information. Thus, incorporating strong augmentations inevitably impose a strong inductive bias that the downstream task requires very little information about the augmentation-related

---

\*Xidian-FIAS International Joint Research Center, 710071, China

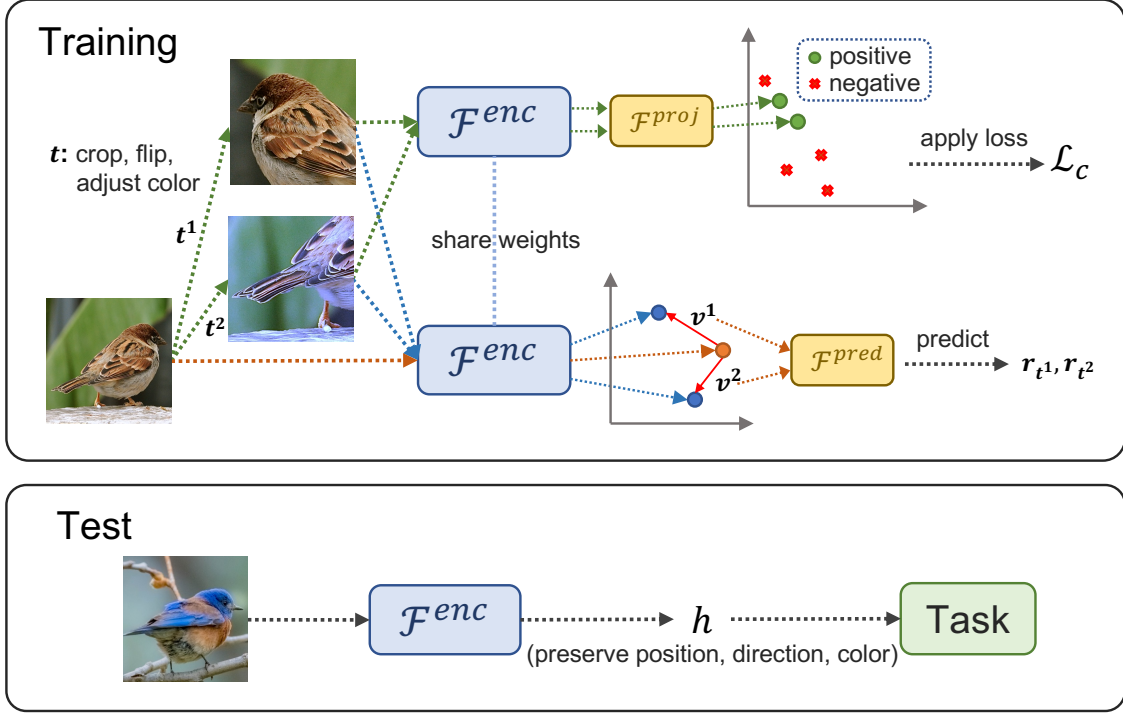


Figure 1: Overview of CIPER. **Top:** During training,  $t^1$  and  $t^2$  are two randomly sampled augmentations.  $\mathcal{F}^{proj}$  and  $\mathcal{F}^{pred}$  are the contrastive and predictive projectors applied on the same encoder  $\mathcal{F}^{enc}$ . The InfoNCE contrastive loss  $\mathcal{L}_c$  is applied to the output of the projector  $\mathcal{F}^{proj}$ . The prediction head  $\mathcal{F}^{pred}$  predicts the parameters of augmentations  $r_{t^1}$  and  $r_{t^2}$  given the difference between the representations of the anchor image and the augmented images in the latent space ( $v^1$  and  $v^2$ ). **Bottom:** During the test phase, the projectors are discarded and the output of the encoder  $h$  is used for downstream tasks. Images are retrieved from [20, 21] under CC BY-SA 4.0 licence.

information contained in the representations. Otherwise, contrastive learning would throw away valuable information [9]. For example, a contrastive learning model would fail when the task is to identify the luminance while the model learns to be invariant to illumination conditions.

On the other hand, equivariant representation learning focuses on learning augmentation-related features [10, 11, 12, 13, 14, 15]. The equivariant representations should change according to the change in the image itself. Much effort has been made to facilitate equivariant representation learning in settings of static images and time series using, respectively, contrastive and predictive learning paradigms. Unlike equivariant contrastive learning, which brings equally-augmented images or frames together [15], predictive learning directly predicts the augmentation parameters (e.g. the transformation matrix if the augmentation is an affine or perspective image transformation [12]). Similar to invariant representation learning using contrastive SSRL, equivariant representations are also prone to bias towards certain features and ignore other information that could be useful for the downstream task. For example, when trained to be equivariant to image rotations, representations of images of cars on roads may focus on the road's direction and ignore the cars in the images. The resulting representations could be helpful when the downstream task is road direction detection. However, this prior knowledge of the task is not known to the model in advance, and this learning paradigm would fail when the task is to identify cars on roads.

One natural solution to this problem is to combine invariant and equivariant features [16, 13, 17, 18, 19]. In this paper, we introduce a method which we call CIPER (Contrastive Invariant and Predictive Equivariant Representation learning) that trains an encoder with two different output heads, one with a contrastive and the other with a predictive objective, to allow both invariant and equivariant features to be extracted. By doing so, learned representations contain information about the invariant semantic meanings that are not influenced by augmentations, as well as information about the factors that are manipulated by the augmentations. This paradigm allows making fuller use of the augmentations without the risk of biasing learning too much towards either augmentation invariant or equivariant features.

## 2 Related Work

### 2.1 Invariant representation learning.

Contrastive learning offers a simple and effective way to encourage representations to be invariant to augmentations. InfoNCE [22] provides a unified categorical cross-entropy loss for identifying positive pairs against negative ones. Recently, SimCLR [5] was proposed to use heavy data augmentations and large batch sizes, leading to better generalization. Keeping the idea of bringing the representations of two augmented versions of one image together, several other methods have also been proposed [23, 24]. ReLIC [25] extends the idea by introducing a regularizer to isolate “style” information. Extending the idea of controlling the separation of “content” and “style,” [26] constructed a simulated dataset and proved that the discarded information in the invariant representation is controlled by the chosen augmentations. Our method extends the conventional contrastive learning method by allowing the preservation of the augmentation-related information.

### 2.2 Equivariant representation learning.

Drawing inspiration from the equivariant map in mathematics, in the field of representation learning with deep neural networks, equivariant representations reflect the transformations applied [27]. Some of these representation learning paradigms encourage the representation space to be mathematically equivariant to the group actions (image transformations) [27, 28, 29]. More generally, methods to learn representations that are equivariant to augmentation parameters such as an image transformation matrix [14, 12], pre-defined tasks such as four-fold rotation prediction [10], and temporal auxiliary tasks for time series [15] have shown competitive performance among other self-supervised learning methods. Another work, Prelax [18], uses residual relaxation and extra augmentations other than those used in SimCLR to encourage representations to include equivariance beyond invariance. Similar to the pretext predictor in Prelax, the prediction head in CIPER predicts all the augmentation parameters given the difference vector between the original image representation and the augmented one. Unlike Prelax, CIPER neither requires a target network, nor extra augmentations, nor residual relaxation, but simply adopts the basic SimCLR setting of network structure and augmentations.

### 2.3 Combining invariant and equivariant learning.

Several methods have been proposed to combine invariant and equivariant representations. Closest to our work are [16, 13, 17, 18, 19]. Specifically, LooC [19] learns a subspace invariant to all but one augmentation for every augmentation and concatenates all subspaces together to form the final representation. However, representations invariant to all but one augmentation do not ensure that they encode the information of that augmentation. Moreover, it requires as many subspaces as augmentations, which may limit the ability to extend to many augmentations. Another work, E-SSL [13], uses a shared backbone network and different heads for either learning invariant features or equivariant representations. They argue that representations should be either invariant or equivariant to a specific augmentation. However, we show that directly predicting the augmentation parameters does not impair the contrastive learning process and provides better performance for downstream tasks. In addition, we do not pick specific augmentations other than those already used in SimCLR while E-SSL chooses an extra four-fold rotation augmentation for the equivariant objective which requires training on 4 extra augmented versions of an image, resulting in a huge training burden. Regarding few-shot learning, a distillation-based method [17] has been developed to learn invariant and equivariant spaces separately and distill them into one feature space. Instead, we found that simply applying both contrastive and predictive objectives simultaneously to learn one feature space allows encoding of invariant and equivariant information naturally without explicit distillation.

## 3 Methods

Given unlabelled high-dimensional data  $x \in \mathbb{R}^m$ , self-supervised representation learning aims at training an encoder network  $\mathcal{F}^{\text{enc}}$  to extract low-dimensional representations  $h = \mathcal{F}^{\text{enc}}(x) \in \mathbb{R}^n$ ,  $n \ll m$ , that should contain useful information for a downstream task target variable  $g$  associated with  $x$ . In other words, the mutual information between the learned representation and the downstream task target variable, i.e.,  $\mathcal{I}(h; g)$  should be maximized. Augmentations are adopted as proxies for downstream tasks regardless of direct learning signals from labels. Augmentations are general transformations  $t \in \mathcal{T}$  that directly operate on raw data  $x$ , resulting in augmented views  $x^t$ . Throughout this work, we refer to a single augmentation  $t$  as a sequence of randomly sampled image operations applied to an image  $x$ . A random augmentation  $t$  can be parameterized by  $r_t$ . For example, suppose that  $t$  consists of two image operations: random cropping at the location  $(i, j)$ , and random horizontal flipping with parameter  $p$  indicating whether the image is

Augmentation	Type	# Dims	Meaning	Setting
Cropping	continuous	4	[location x, location y, height, width]	$p = 1$ ; scale: (0.2, 1.0)
Horizontal Flip	binary	1	0 for not flipped, 1 otherwise	$p = 0.8$
Color Jittering	continuous	4	[brightness, contrast, saturation, hue]	$p = 0.8$
Grayscale	binary	1	0 for grayscale, 1 otherwise	$p = 0.2$

Table 1: Image augmentations and their parameters. Parameter  $p$  indicates the probability of applying a particular augmentation. Binary parameters refer to the probability itself. Parameters of continuous parameters are randomly drawn and returned using the TorchVision package [30].

horizontally flipped. Then  $r_t = [i, j, p]$ . Throughout the paper, chosen augmentations are performed in a fixed order (See Sect. 4 for details).

### 3.1 Invariant Contrastive Learning.

Contrastive learning promotes representations that are invariant to data augmentations. For a given data point  $x_i$  which we call an anchor, contrastive learning defines the positive samples as the differently augmented versions of the anchor  $x_i$ , resulting in  $x_i^{t_1}$  and  $x_i^{t_2}$ , and negative samples as different data points with different augmentations  $x_j^{t_1}$  and  $x_j^{t_2}$ . There could be more than a pair of positive samples, but as we adopt the SimCLR framework in CIPER, we only consider one pair of positive samples of a given anchor. Then the objective of contrastive learning is to maximize the similarities between corresponding representations of the positive pairs and minimize the similarities between positive samples and negative samples. In SimCLR, a batch of  $N$  data points are sampled and augmented twice, resulting in pairs of augmented views. The input image pairs are then put through the encoder  $\mathcal{F}^{\text{enc}}$ , resulting in representations  $h_i$ . The representations are further projected through a projection head  $\mathcal{F}^{\text{proj}}$  to  $z$  where the InfoNCE loss is applied. We denote the contrastive loss as  $\mathcal{L}_c$ . If the training fully converges, which generally does not occur in real cases, then there should be no way to distinguish  $z_i^{t_1}$ ,  $z_i^{t_2}$  and  $z_i$ . Although the loss function is not directly applied to  $h$ ,  $h$  should generally be influenced the same way as  $z$ . Hence the loss function should reduce the information in the representations to reflect as little as possible the augmentations applied. However, we show in Sect. 4 that this contrastive learning objective does preserve the augmentation information in some cases. In other words,  $\mathcal{I}(\mathcal{F}^{\text{enc}}(x^t); t)$  is not fully minimized. Moreover, there is no guarantee that decreasing  $\mathcal{I}(\mathcal{F}^{\text{enc}}(x^t); t)$  necessarily results in an increase in  $\mathcal{I}(\mathcal{F}^{\text{enc}}(x^t); g)$ , given no prior knowledge about how the augmentation  $t$  affects the performance on task  $g$ .

### 3.2 Equivariant Predictive Learning.

Inspired by the equivariant map in mathematics, equivariant representations discussed here change according to the input data. In other words, whether the information of the input data is preserved is of less concern as long as the representation reflects how the data changes due to the image augmentations. Considering this definition through the lens of mutual information, equivariant representation learning tries to maximize  $\mathcal{I}(\mathcal{F}^{\text{enc}}(x^t); t)$ , where  $\mathcal{F}^{\text{enc}}$  is the encoder coupled with an additional prediction head and prediction loss. As stated in Sect. 3.1, increasing  $\mathcal{I}(\mathcal{F}^{\text{enc}}(x^t); t)$  may as well increase  $\mathcal{I}(\mathcal{F}^{\text{enc}}(x^t); g)$  since the augmentation  $t$  could potentially change the performance on task  $g$ . By parameterizing the augmentations, this can be easily done by maximizing  $\mathcal{I}(\mathcal{F}^{\text{enc}}(x^t); r_t)$ . Specifically, we adopt static image augmentations with parameters as shown in Tab. 3.1. These augmentations are the same as those used in SimCLR. The total number of dimensions of static image augmentations is 10. We also experiment with dataset-provided special augmentations for specific datasets, which will be elaborated in Sect. 4. In CIPER, we maximize  $\mathcal{I}(\mathcal{F}(x^t); r_t)$  by simply adding a predictor  $\mathcal{F}^{\text{pred}}$  on top of the same encoder  $\mathcal{F}^{\text{enc}}$  to predict the parameters of the augmentations. While other choices may be possible, we find this auxiliary prediction head and prediction objective is the most straightforward and implementation-friendly way. We also use the same augmentation paradigm as in Sec. 3.1, i.e., augmenting each image twice as a pair. Specifically, taking an anchor image  $x_i$  and one augmented image  $x_i^{t_1}$  for example, the prediction head  $\mathcal{F}^{\text{proj}}$  takes the difference between the representations of the anchor image  $x_i$  and the augmented image  $x_i^{t_1}$ , i.e.,  $h_i - h_i^{t_1}$  as input. The output of the prediction head is directly fed into the prediction objective. To maintain simplicity, for static image augmentations, we normalize the prediction target (the augmentation parameters) across the batch dimension and apply a simple MSE loss:

$$\mathcal{L}_p = - \frac{\sum_i^N \left( \sum_k^M \left( r_{t_i^1}^k - z_{t_i^1}^k \right)^2 + \sum_k^M \left( r_{t_i^2}^k - z_{t_i^2}^k \right)^2 \right)}{2 \cdot N \cdot M}, \quad (1)$$

where  $M$  is the total number of dimensions of the augmentations and  $N$  is the batch size. For other dataset-provided augmentations, the loss applied depends on the type of the augmentation parameter. Specifically, we adopt a cross-entropy loss for categorical augmentation parameters and an MSE loss for continuous augmentation parameters.

### 3.3 Combining Invariant and Equivariant Representations.

As stated before, either only decreasing  $\mathcal{I}(\mathcal{F}^{\text{enc}}(x^t); t)$  or only increasing  $\mathcal{I}(\mathcal{F}^{\text{enc}}(x^t); t)$  may not suffice to perform well on a particular downstream task. Therefore, we simultaneously apply the invariance-encouraging InfoNCE loss to the projection output  $z_i^c$  and the equivariance-encouraging objective (Eq. 1) to the prediction output  $z_i^e$ . Notice that unlike in Eq. 1, where only the predictive objective is applied, here  $z_i^c$  differs from  $z_i^e$ . The total loss is then:

$$\mathcal{L} = \mathcal{L}_c + \alpha \cdot \mathcal{L}_p, \quad (2)$$

where  $\alpha$  is the weighting hyper-parameter of the predictive loss. We use  $\alpha = 1.0$  for CIPER in all experiments except for the ablation study. After training, both heads are discarded and we only use the encoder to encode the data into representations  $h$ . Although combining two counteracting objectives seems counter-intuitive, the results shown in 4.2 suggest that the representations benefit from both invariance and equivariance.

## 4 Experiments

### 4.1 Datasets, Augmentations, Experimental Setup.

We validate our method on CIFAR10 [31] for image classification. In addition, we test our method using two additional image datasets which offer specific time-based augmentations, namely CORE50 [32] and TDW [33]. CORE50 comprises videos of common objects (cups, balls, phones, etc.) that are manipulated in different environments (kitchen, garden, etc.) referred to as sessions (See Fig. 3 for example frames). Importantly, only 2 sessions are used as the training set and the remaining 9 sessions are used as test set. The reason for this skewed split is that the session information is rather easy to encode and can result in around 80% classification accuracy with a randomly initialized network even with this split. The TDW environment comprises sequences of views of computer rendered objects seen from different perspectives. For TDW, we follow the training/test set split defined in [33]. Dealing with CORE50 and TDW, one typical additional augmentation [33] is sampling the next image in the sequence of views as the positive pair. This time-based augmentation aims to make the latent representations of successive views (positive pairs) more similar when we train with the contrastive objective. However, this type of augmentation lacks the ability to be parameterized. Thus, we define new augmentations by utilizing the flexibility to manipulate the viewing points and sessions. Specifically, in TDW, the view of an object can be manipulated in 3 dimensions (azimuth, elevation, and distance). We treat the session of the CORE50 dataset as categorical parameters with 11 categories (2 for training) and the amount of change in view for TDW as a 3-dimensional continuous parameter vector. We refer these dataset-specific augmentations to ‘‘Dataset Aug.’’ in Tab. 4.1. We also test the traditional image transformation-based augmentations on CORE50 and TDW, which we denote as ‘‘Image Aug.’’. For image transformation-based augmentations, we adopt the four augmentations listed in Tab. 3.1 in the same order as given in the table, following the standard SimCLR implementation. Experiments of ablations on these augmentations are also conducted for CIFAR10. We also compare the performance of using dataset-specific augmentations with the performance of image augmentations.

In our experiments, we adopt ResNet18 [34] as our backbone encoder structure. The first convolutional kernel size is set to 3, and the first max pooling layer is removed, following the setting of SimCLR [5]. According to the setting of E-SSL [13], the projection head following the encoder is a two-layered MLP [35] with a hidden layer consisting of 2048 hidden units followed by a batch normalization layer [36] and a ReLU [37] activation function. The final layer of the MLP also has 2048 units followed by a batch normalization layer. The predictor of the predictive network is also a two-layered MLP with 512 hidden units followed by a LayerNorm [38] layer and ReLU activation function. The output dimension of the predictor varies according to the dimension of augmentation parameters to be predicted. Details of the augmentations are elaborated in Tab. 3.1. Regarding the implementation of random augmentations, we use the official TorchVision [30] implementation with a wrapper providing the random parameters used for the augmentations. To facilitate easier encoding of relative position information for the encoder, we adopt the positional encoding proposed in [39] by concatenating two-dimensional Cartesian coordinates alongside the RGB-channels. The learning rate, which starts from 0.03, decays to 0 using a cosine decay scheduler with no warmup session. We use an SGD optimizer with  $5 \times 10^{-4}$  weight decay and 0.9 momentum. We train both networks for 800 epochs with a batch size of 256 on CIFAR10 using the loss functions from Sec. 3. For TDW and CoRE50, we train for 100 epochs with a batch size of 64. After training, we evaluate the performance of the encoders following the standard linear evaluation protocol in SimCLR. Specifically, for CIFAR10, we freeze the parameters in the encoder and train a linear layer on top of the encoder using the training data and evaluate the linear classification accuracy on the test dataset. For TDW and

Method	CORE50 (Obj Acc.)	TDW (Obj Acc.)	CORE50 (Sess Acc.)	TDW (View Err.)
Random encoder	18.44 $\pm$ 10.01	60.73 $\pm$ 8.39	81.29 $\pm$ 5.51	37.07 $\pm$ 0.52
Contrastive w/ Image Aug.	66.95 $\pm$ 0.84	95.91 $\pm$ 0.17	99.08 $\pm$ 0.09	40.88 $\pm$ 1.38
Contrastive w/ Dataset Aug.	60.55 $\pm$ 0.87	98.32 $\pm$ 0.15	96.81 $\pm$ 0.61	40.84 $\pm$ 2.69
CIPER w/ Image Aug.	<b>75.43 <math>\pm</math> 0.61</b>	97.36 $\pm$ 0.16	<b>99.97 <math>\pm</math> 0.02</b>	29.63 $\pm$ 1.71
CIPER w/ Dataset Aug.	67.46 $\pm$ 0.41	<b>98.92 <math>\pm</math> 0.41</b>	99.72 $\pm$ 0.07	<b>6.48 <math>\pm</math> 0.15</b>

Table 2: CORE50 and TDW Results. The object and session classification accuracy (%) are referred to as Obj Acc. and Sess Acc., respectively. For TDW dataset, we mark the regression error of the view as View Err. Regular image-based augmentations and dataset-specific augmentations are marked as Image Aug. and Data Aug. Each reported value is shown as mean  $\pm$  std across 5 runs.

CORE50, we also train a regressor/classifier to identify the view/session. In the case of CORE50, both training and test sets for the linear session classifier are sampled from the 9 unseen sessions. The linear classifiers and the regressor are trained for 100 epochs using an SGD optimizer with  $10^{-6}$  weight decay and 0.9 Nesterov momentum [40, 41]. The learning rate for training the linear classifier starts at 1 and decays by a factor of 3.33 every 10 epochs. We repeat the whole training-evaluation process for each experiment five times with different random seeds and report the mean accuracy and standard deviations.

## 4.2 Results

We evaluate our encoder on CIFAR10 with the contrastive objective and with CIPER, which uses both contrastive and predictive objectives (Tab. 4.2). The encoder trained with the predictive network alone can not match the performance of the state-of-the-art contrastive learning methods. However, by combining both contrastive and predictive objects CIPER achieves better performance on the CIFAR10 dataset compared with our re-implementation of the SimCLR baseline. This shows that CIPER better utilizes the information provided by the augmentations. Furthermore, we evaluate CIPER on the CORE50 and TDW datasets, which offer additional augmentation choices. We also report the results of classifying the session in CORE50 and regression on the view parameters of TDW datasets. From the results shown in Tab. 4.1 we observe that dataset-specific augmentations can achieve better performance than general image-based augmentations. We further find that when dealing with dataset-specific augmentations, the contrastive representations would fail to achieve high session classification accuracy and low view identification error, while CIPER can solve this problem and improve the contrastive method on other tasks. This shows that CIPER is robust to situations where one of the two objectives alone would fail. These findings show that the combined CIPER objective retains rich information about the augmentations compared to the invariant objective alone. Another interesting finding is that compared with the untrained randomly-initialized encoder, the contrastive representations achieve higher session classification accuracy on CORE50. This finding supports our assumption that the invariant representations generally discard the information about the augmentation and the equivariant representations do the opposite, while neither of them achieve the goal of discarding or preserving augmentation information completely. CIPER combines these two objectives to robustly preserve rich information.

Method	Acc.
SimCLR (2 $\times$ )	91.1
SimCLR (re-production) (2 $\times$ )	91.7 $\pm$ 0.1
E-SSL (6 $\times$ )	94.1 $\pm$ 0.0
Predictive (3 $\times$ )	53.4 $\pm$ 2.3
CIPER (3 $\times$ )	92.2 $\pm$ 0.3

Table 3: Linear classification accuracy (%) on CIFAR10. The “(n $\times$ )” means that n augmented/original images are used for one image sample during training. For a fair comparison, only the methods with the SimCLR backbone are shown. The results of SimCLR and E-SSL are retrieved from [13].

In Fig. 2 we visualize the learned representations. We use PacMap [42] to reduce the dimension of the representations to 2, revealing a clustering of learned representations with the contrastive and the full CIPER objective on TDW. We can see that the contrastive objective drives representations to form compact clusters of objects, while the CIPER objective also encodes some structure related to the augmentations. To further illustrate what the networks pay attention to, we adopt FullGrad [43] on CORE50 using the dataset-specific augmentation and the linear object classifier obtained at test phase to generate saliency maps as shown in Fig.3. Counter-intuitively, although CIPER generally focuses on the surroundings while SimCLR pays attention to the objects, the object classification accuracy of CIPER is higher than SimCLR (see Tab. 4.1). The reason of this finding remains unclear and requires further research. In addition,

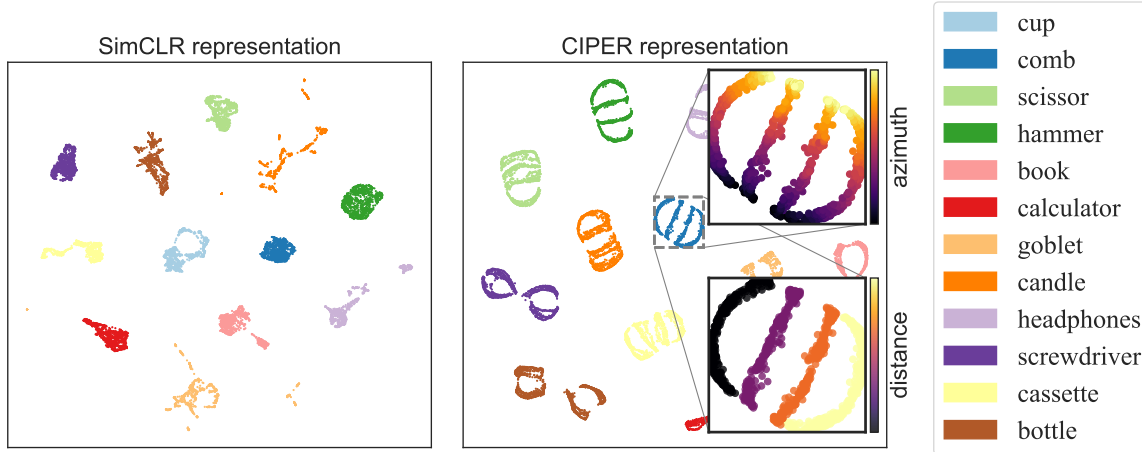


Figure 2: PacMap [42] representation visualizations of the TDW dataset after 100 epochs of training with dataset-specific augmentations. **Left:** representations with SimCLR objective. **Right:** representations with CIPER objective. Note how CIPER encodes view point information without losing the ability to cluster representations of the same object.

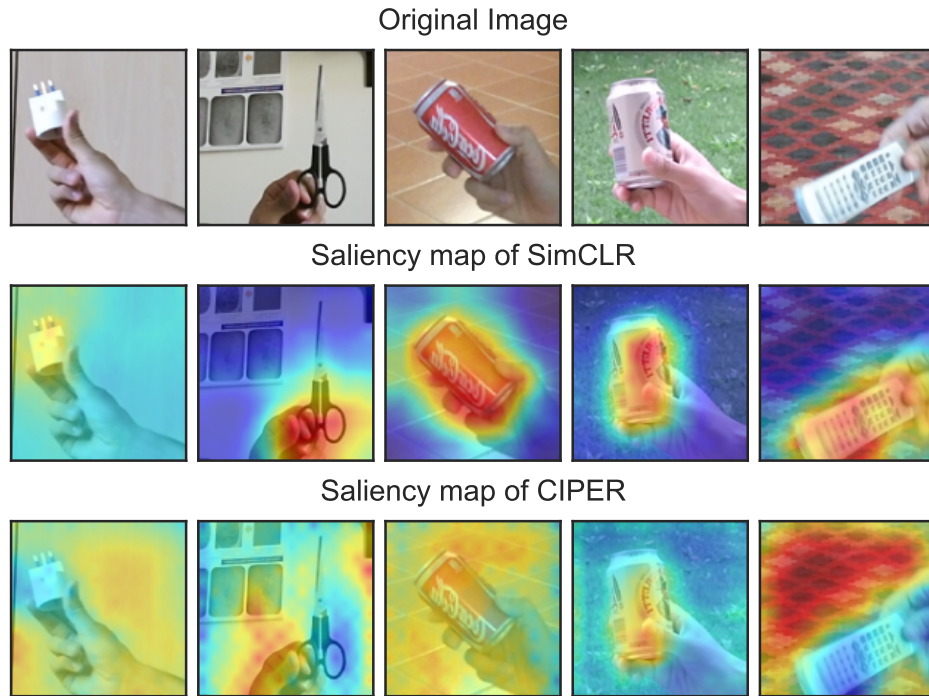


Figure 3: Example FullGrad [43] saliency maps of images from the CORE50 dataset for the encoders trained with SimCLR and CIPER (ours). The augmentations used are the data-specific augmentation defined in 4.1.

this finding shows that CIPER could potentially be utilized to learn disentangled representations of objects against backgrounds.

To study what augmentations contribute most to the downstream classification task when training with CIPER, we remove each augmentation and test the performance. Similar to the findings in [5], our results on the left in Fig.4 show that every augmentation benefits the downstream task while random cropping and color jittering contribute the most to the performance. Limitations to this ablation study are that augmentations could potentially interact with each other when applied in different orders and influence the final performance. Due to the combinatorial complexity of studying these interactions and potentially many other augmentations, we only perform a single removal test of the

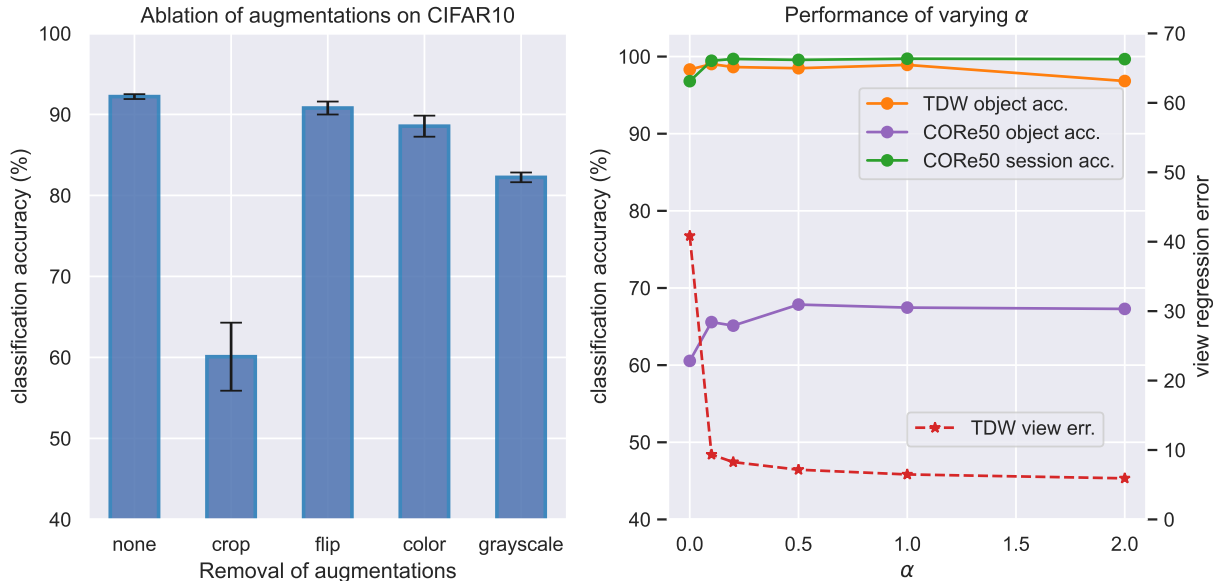


Figure 4: Ablation study of single augmentation removal and varying  $\alpha$ . **Left:** CIFAR10 object classification accuracy with each augmentation removed. **Right:** Object/Session classification accuracy on TDW and CORE50 is marked as solid lines and view regression error on TDW is noted as the dotted line.

augmentations used in SimCLR and our experiments. Further more, to study the impact of the prediction head, we vary the weighting hyper-parameter  $\alpha$  and conducted experiments on TDW and CORE50. Results are shown on the right in Fig.4. It can be observed that increasing  $\alpha$  can lead to higher object classification accuracy on both TDW and CORE50, as well as higher session classification accuracy and lower view regression error on CORE50 and TDW, respectively. However, the classification accuracy may drop if  $\alpha$  is too high and we set  $\alpha = 1$  as default for other experiments in Sect. 4.

## 5 Discussion

We have proposed a new method (CIPER) for combining invariant and equivariant objectives in self-supervised representation learning. Invariance is promoted via the popular SimCLR method. Equivariance, we adopted a prediction approach that learns to estimate the parameters of the augmentations applied to the input data. In the test phase, the output heads are simply discarded and the encoder is used for downstream tasks. One explanation of two counteracting objectives to work together could be that the representations can contain identity-preserving information with semantic meaning, which augmentations do not alter, as well as augmentation-related information at the same time, while the two heads extract invariant and equivariant information. Experiments show the benefits of our method compared to similar state-of-the-art works. Further results show that in some situations where the standard contrastive learning method is not enough, the incorporation of the complementary equivariant objective of CIPER improves the representation.

Interestingly, the combination of invariant and equivariant representation learning objectives used in CIPER is reminiscent of the separation of the primate visual system into a so-called ventral or “what” stream for invariant object recognition and a so-called dorsal or “where/how” stream for physical interaction with objects. This may reflect a general design principle for versatile vision systems capable of supporting qualitatively different downstream tasks.

## 6 Acknowledgements

This research was supported by the research group ARENA (Abstract Representations in Neural Architectures) of the Deutsche Forschungsgemeinschaft (DFG) under grant agreement TR 881/10-1. We also acknowledge support by “The Adaptive Mind” and “The Third Wave of Artificial Intelligence,” funded by the Excellence Program of the Hessian Ministry of Higher Education, Science, Research and Art. JT is supported by the Johanna Quandt foundation.



## References

- [1] Alexander Kolesnikov, Xiaohua Zhai, and Lucas Beyer. Revisiting self-supervised visual representation learning. In *Proceedings of the IEEE/CVF conference on computer vision and pattern recognition*, pages 1920–1929, 2019.
- [2] Aleksandr Ermolov, Aliaksandr Siarohin, Enver Sangineto, and Nicu Sebe. Whitening for self-supervised representation learning. In *International Conference on Machine Learning*, pages 3015–3024. PMLR, 2021.
- [3] Xiao Liu, Fanjin Zhang, Zhenyu Hou, Li Mian, Zhaoyu Wang, Jing Zhang, and Jie Tang. Self-supervised learning: Generative or contrastive. *IEEE Transactions on Knowledge and Data Engineering*, 2021.
- [4] Hanwen Liang, Niamul Quader, Zhixiang Chi, Lizhe Chen, Peng Dai, Juwei Lu, and Yang Wang. Self-supervised spatiotemporal representation learning by exploiting video continuity. In *Proceedings of the AAAI Conference on Artificial Intelligence*, volume 36, pages 1564–1573, 2022.
- [5] Ting Chen, Simon Kornblith, Mohammad Norouzi, and Geoffrey Hinton. A simple framework for contrastive learning of visual representations. In *International conference on machine learning*, pages 1597–1607. PMLR, 2020.
- [6] Xinlei Chen and Kaiming He. Exploring simple siamese representation learning. In *Proceedings of the IEEE/CVF Conference on Computer Vision and Pattern Recognition*, pages 15750–15758, 2021.
- [7] Michael Laskin, Aravind Srinivas, and Pieter Abbeel. Curl: Contrastive unsupervised representations for reinforcement learning. In *International Conference on Machine Learning*, pages 5639–5650. PMLR, 2020.
- [8] Alec Radford, Jong Wook Kim, Chris Hallacy, Aditya Ramesh, Gabriel Goh, Sandhini Agarwal, Girish Sastry, Amanda Askell, Pamela Mishkin, Jack Clark, et al. Learning transferable visual models from natural language supervision. In *International Conference on Machine Learning*, pages 8748–8763. PMLR, 2021.
- [9] Julius Von Kügelgen, Yash Sharma, Luigi Gresele, Wieland Brendel, Bernhard Schölkopf, Michel Besserve, and Francesco Locatello. Self-supervised learning with data augmentations provably isolates content from style. *Advances in neural information processing systems*, 34:16451–16467, 2021.
- [10] Spyros Gidaris, Praveer Singh, and Nikos Komodakis. Unsupervised Representation Learning by Predicting Image Rotations. *arXiv e-prints*, March 2018.
- [11] Spyros Gidaris, Andrei Bursuc, Nikos Komodakis, Patrick Pérez, and Matthieu Cord. Boosting few-shot visual learning with self-supervision. In *Proceedings of the IEEE/CVF international conference on computer vision*, pages 8059–8068, 2019.
- [12] Liheng Zhang, Guo-Jun Qi, Liqiang Wang, and Jiebo Luo. Aet vs. aed: Unsupervised representation learning by auto-encoding transformations rather than data. In *Proceedings of the IEEE/CVF Conference on Computer Vision and Pattern Recognition*, pages 2547–2555, 2019.
- [13] Rumén Dangovski, Li Jing, Charlotte Loh, Seungwook Han, Akash Srivastava, Brian Cheung, Pulkit Agrawal, and Marin Soljačić. Equivariant Contrastive Learning. *arXiv e-prints*, October 2021.
- [14] Zeyu Feng, Chang Xu, and Dacheng Tao. Self-supervised representation learning by rotation feature decoupling. In *Proceedings of the IEEE/CVF Conference on Computer Vision and Pattern Recognition*, pages 10364–10374, 2019.
- [15] Simon Jenni and Hailin Jin. Time-equivariant contrastive video representation learning. In *Proceedings of the IEEE/CVF International Conference on Computer Vision*, pages 9970–9980, 2021.
- [16] Liheng Zhang. *Equivariance and Invariance for Robust Unsupervised and Semi-Supervised Learning*. PhD thesis, University of Central Florida, 2020.
- [17] Mamshad Nayeem Rizve, Salman Khan, Fahad Shahbaz Khan, and Mubarak Shah. Exploring complementary strengths of invariant and equivariant representations for few-shot learning. In *Proceedings of the IEEE/CVF Conference on Computer Vision and Pattern Recognition*, pages 10836–10846, 2021.
- [18] Yifei Wang, Zhengyang Geng, Feng Jiang, Chuming Li, Yisen Wang, Jiansheng Yang, and Zhouchen Lin. Residual relaxation for multi-view representation learning. *Advances in Neural Information Processing Systems*, 34:12104–12115, 2021.
- [19] Tete Xiao, Xiaolong Wang, Alexei A. Efros, and Trevor Darrell. What Should Not Be Contrastive in Contrastive Learning. *arXiv e-prints*, August 2020.
- [20] Pranav Tadepalli. English: A Western Bluebird sitting on a branch at in Los Gatos, California., March 2021.
- [21] Claudio Gennari from Roma Italia. English: Italian Sparrow pair, January 2009.

- [22] Aaron van den Oord, Yazhe Li, and Oriol Vinyals. Representation Learning with Contrastive Predictive Coding. *arXiv e-prints*, July 2018.
- [23] Kaiming He, Haoqi Fan, Yuxin Wu, Saining Xie, and Ross Girshick. Momentum contrast for unsupervised visual representation learning. In *Proceedings of the IEEE/CVF conference on computer vision and pattern recognition*, pages 9729–9738, 2020.
- [24] Adrien Bardes, Jean Ponce, and Yann LeCun. VICReg: Variance-Invariance-Covariance Regularization for Self-Supervised Learning. *arXiv e-prints*, page arXiv:2105.04906, May 2021.
- [25] Jovana Mitrovic, Brian McWilliams, Jacob Walker, Lars Buesing, and Charles Blundell. Representation Learning via Invariant Causal Mechanisms. *arXiv e-prints*, October 2020.
- [26] Julius von Kügelgen, Yash Sharma, Luigi Gresele, Wieland Brendel, Bernhard Schölkopf, Michel Besserve, and Francesco Locatello. Self-Supervised Learning with Data Augmentations Provably Isolates Content from Style. *arXiv e-prints*, June 2021.
- [27] Taco Cohen and Max Welling. Group equivariant convolutional networks. In Maria Florina Balcan and Kilian Q. Weinberger, editors, *Proceedings of The 33rd International Conference on Machine Learning*, volume 48 of *Proceedings of Machine Learning Research*, pages 2990–2999, New York, New York, USA, 20–22 Jun 2016. PMLR.
- [28] Jyri J. Kivinen and Christopher K. I. Williams. Transformation equivariant boltzmann machines. In Timo Honkela, Włodzisław Duch, Mark Girolami, and Samuel Kaski, editors, *Artificial Neural Networks and Machine Learning – ICANN 2011*, pages 1–9, Berlin, Heidelberg, 2011. Springer Berlin Heidelberg.
- [29] Daniel E. Worrall, Stephan J. Garbin, Daniyar Turmukhambetov, and Gabriel J. Brostow. Harmonic networks: Deep translation and rotation equivariance. In *Proceedings of the IEEE Conference on Computer Vision and Pattern Recognition (CVPR)*, pages 5028–5037, July 2017.
- [30] Sébastien Marcel and Yann Rodriguez. Torchvision the machine-vision package of torch. In *Proceedings of the 18th ACM international conference on Multimedia*, pages 1485–1488, 2010.
- [31] Alex Krizhevsky. Learning multiple layers of features from tiny images. Technical report, Computer Science, University of Toronto, 2009.
- [32] V Lomanco and Davide Maltoni. Core50: a new dataset and benchmark for continual object recognition. In *Proceedings of the 1st Annual Conference on Robot Learning*, pages 17–26, 2017.
- [33] Felix Schneider, Xia Xu, Markus R. Ernst, Zhengyang Yu, and Jochen Triesch. Contrastive learning through time. In *SVRHM 2021 Workshop @ NeurIPS*, pages 1–14, 2021.
- [34] Kaiming He, Xiangyu Zhang, Shaoqing Ren, and Jian Sun. Deep residual learning for image recognition. In *Proceedings of the IEEE conference on computer vision and pattern recognition*, pages 770–778, 2016.
- [35] David E Rumelhart, Geoffrey E Hinton, and Ronald J Williams. Learning internal representations by error propagation. Technical report, California Univ San Diego La Jolla Inst for Cognitive Science, 1985.
- [36] Sergey Ioffe and Christian Szegedy. Batch normalization: Accelerating deep network training by reducing internal covariate shift. In *International conference on machine learning*, pages 448–456. PMLR, 2015.
- [37] Vinod Nair and Geoffrey E. Hinton. Rectified linear units improve restricted boltzmann machines. In Johannes Fürnkranz and Thorsten Joachims, editors, *Proceedings of the 27th International Conference on Machine Learning (ICML-10)*, June 21–24, 2010, Haifa, Israel, pages 807–814. Omnipress, 2010.
- [38] Jimmy Lei Ba, Jamie Ryan Kiros, and Geoffrey E. Hinton. Layer Normalization. *arXiv e-prints*, July 2016.
- [39] Rito Murase, Masanori Suganuma, and Takayuki Okatani. How can CNNs use image position for segmentation? *arXiv e-prints*, May 2020.
- [40] Ilya Sutskever, James Martens, George Dahl, and Geoffrey Hinton. On the importance of initialization and momentum in deep learning. In *International conference on machine learning*, pages 1139–1147. PMLR, 2013.
- [41] Yurii Nesterov. A method for solving the convex programming problem with convergence rate  $o(1/k^2)$ . *Proceedings of the USSR Academy of Sciences*, 269:543–547, 1983.
- [42] Yingfan Wang, Haiyang Huang, Cynthia Rudin, and Yaron Shaposhnik. Understanding how dimension reduction tools work: An empirical approach to deciphering t-sne, umap, trimap, and pacmap for data visualization. *J. Mach. Learn. Res.*, 22(201):1–73, 2021.
- [43] Suraj Srinivas and François Fleuret. Full-gradient representation for neural network visualization. *Advances in neural information processing systems*, 32, 2019.